Featured Article

Amyloid beta synaptotoxicity is Wnt–planar cell polarity dependent and blocked by fasudil

Katherine J. Sellers[a,1], Christina Elliott[a,1], Joshua Jackson[b,1], Anshua Ghosh[a,1], Elena Ribe[c],
Ana Rojo-Sanchís[d], Heledd H. Jarosz-Griffiths[e], Iain A. Watson[a], Weiming Xia[f],
Mikhail Semenov[f], Peter Morin[f], Nigel M. Hooper[e], Rod Porter[g], Jane Preston[h], Raya Al-Shawi[i],
George Baillie[j], Simon Lovestone[c], Antonio Cuadrado[d], Michael Harte[b], Paul Simons[i],
Deepak P. Srivastava[a,**], Richard Killick[a,*]

[a]Maurice Wohl Clinical Neuroscience Institute, King's College London, London, UK
[b]Faculty of Biology, Medicine and Health, Division of Pharmacy and Optometry, University of Manchester, Manchester, UK
[c]Department of Psychiatry, Warneford Hospital, University of Oxford, Oxford, UK
[d]Instituto de Investigaciones Biomédicas "Alberto Sols", Madrid University, Madrid, Spain
[e]Faculty of Biology, Medicine and Health, Division of Neuroscience and Experimental Psychology, University of Manchester, Manchester, UK
[f]New England Geriatric Research Education and Clinical Center, Boston University School of Medicine, Boston, MA, USA
[g]Rod Porter, Rod Porter Consultancy, Baldock, England, UK
[h]Institute of Pharmaceutical Science, King's College London, London, UK
[i]Centre for Amyloidosis and Acute Phase Proteins, Royal Free Campus, University College London, London, UK
[j]Institute of Cardiovascular and Medical Science, University of Glasgow, Glasgow, Scotland, UK

Abstract

Introduction: Synapse loss is the basis of the cognitive decline indicative of dementia. In the brains of Alzheimer's disease (AD) sufferer's amyloid beta (Aβ) peptides aggregate to form senile plaques but as soluble peptides that are toxic to synapses. We previously demonstrated that Aβ induces Dickkopf-1 (Dkk1), which in turn activates the Wnt–planar cell polarity (Wnt-PCP) pathway to drive tau pathology and neuronal death.

Methods: We compared the effects of Aβ and Dkk1 on synapse morphology and memory impairment while inhibiting or silencing key elements of the Wnt-PCP pathway.

Results: We demonstrate that Aβ synaptotoxicity is also Dkk1 and Wnt-PCP dependent, mediated by the arm of Wnt-PCP regulating actin cytoskeletal dynamics via Daam1, RhoA, and ROCK, and can be blocked by the drug fasudil.

Discussion: Our data place Wnt-PCP signaling at the center of AD neuropathology and indicate that fasudil could be repositioned as a treatment for AD.

© 2017 Published by Elsevier Inc. on behalf of the Alzheimer's Association. This is an open access article under the CC BY license (http://creativecommons.org/licenses/by/4.0/).

Keywords: Dickkopf-1; Amyloid; Synapse; Synaptotoxicity; Wnt; Planar cell polarity; ROCK; DAAM1; Fasudil; Alzheimer's

1. Background

Amyloid beta (Aβ) has long been associated with Alzheimer's disease (AD) through a propensity to form insoluble deposits, senile plaques, a hallmark of the AD brain. Overwhelming genetic and experimental evidence indicate that Aβ and its parent molecule, the amyloid precursor

protein (APP), are key players in the neuropathogenic processes driving AD. Aβ readily self-associates to form a range of soluble oligomers and insoluble fibers, and the current consensus view holds that these are the small soluble oligomeric forms of Aβ rather than the plaques themselves that are the neurotoxic species [1–3]. We have previously found that Aβ-driven increases in tau phosphorylation (a second hallmark of the disease) and neuronal death are dependent on activation of a branch of Wingless/Wnt signaling known as the Wnt–planar cell polarity (Wnt-PCP) pathway, specifically the arm of Wnt-PCP acting through JNK and its target c-Jun to regulate gene transcription [4]. We have shown that Aβ activates Wnt-PCP through the ability of Aβ to induce Dickkopf-1 (Dkk1), which by blocking the binding interaction between LRP6 and frizzled prevents canonical Wnt–β-catenin activity and concomitantly activates Wnt-PCP signaling [5,6]. Furthermore, our data indicate that Dkk1 and Wnt-PCP shape the transcriptomic profile of the AD brain and the activity of pathways within it most associated with the disease [4,7]. The top four most significant of these pathways being the Adherens Junction, Wnt signaling, TGF-β signaling, and LTP, which are all intimately involved in synaptic plasticity [8–10].

Aβ synaptotoxicity is thought to be a very early event in the disease process, central to disease etiology, and possibly the driver of many other neurotoxic properties attributed to Aβ [2,11,12]. Indeed, the degree of cognitive impairment in AD correlates more closely with synapse number than with amyloid load or extent of tau pathology [2,13,14]. However, although widely studied, the underlying mechanisms of Aβ synaptotoxicity have yet to be fully determined [2,15].

The synaptic effects of Aβ have been reported to be Dkk1 dependent [16]. In addition to influencing transcription via JNK/c-Jun, the Wnt-PCP pathway also regulates cytoskeletal dynamics through ras homolog family member A (RhoA) and rho-associated coiled-coil containing protein kinase (ROCK), two key regulators of synapse formation [17,18], shown to be responsive to Aβ [19]. Given this, we investigated the possibility that Aβ may exert its synaptotoxicity by activating the Wnt-PCP/RhoA/ROCK pathway and present evidence that this is the case. Furthermore, we have evaluated the potential of the ROCK inhibitor drug, fasudil, as a therapeutic approach to ameliorate both the synaptic and cognitive effects of Aβ.

2. Methods

2.1. Dkk1 measures

Rat Dkk1 messenger RNA expression was performed by *quantitative RT-PCR* and protein levels determined using a DuoSet enzyme-linked immunosorbent assay Kit (R&D Systems, DY1906), both as previously described [4].

2.2. Neuronal culture and transfections

Primary cortical neuronal cultures were prepared from Sprague-Dawley rat E18 embryos as described previously [20]. Cells were seeded onto coverslips coated with poly-D-lysine (0.2 mg/mL, Sigma), at a density of 3×10^5/well equating to 857/mm^2. Cells were cultured in feeding media: neurobasal medium (21103049) supplemented with 2% B27 (17504044), 0.5 mM glutamine (25030024), and 1% penicillin/streptomycin (15070063) (all reagents from Life technologies, UK). After 4 days in vitro (DIV) 200 μM D,L-aminophosphonovalerate (ab120004; Abcam) was added to media to maintain neuronal health over long-term culture and to reduce cell death because of excitotoxicity [20]. Fifty percent media changes were performed twice weekly until desired time in culture was reached (DIV 23). Cells were then transfected with an eGFP expression construct driven by the synapsin 1 promoter using Lipofectamine 2000. Transfections were allowed to proceed for 2 days, resulting in 5% to 10% transfection efficacy [20,21].

2.3. Pharmacologic treatments of neuronal cultures

All pharmacologic treatments were performed in artificial cerebral spinal fluid: 125 mM NaCl, 2.5 mM KCL, 26.2 mM NaHCO$_3$, 1 mM NaH$_2$PO$_4$, 11 mM glucose, 5 mM Hepes, 2.5 mM CaCl$_2$, 1.25 mM MgCl$_2$, and 0.2 mM aminophosphonovalerate. Neuronal cultures were pretreated with inhibitor compounds for 30 minutes before application of Dkk1 recombinant protein, Aβ$_{1-42}$ oligomers (AβO), or fibrillar Aβ$_{25-35}$ to culture media. All compounds were dissolved in water or DMSO at a concentration of 10 or 1 mM, and serially diluted to a 10 times working concentration in artificial cerebral spinal fluid and applied directly to neuronal cultures. Final concentration of solvent was <0.01%, as also used in vehicle control. Treatments were allowed to proceed for indicated times before being fixed for immunocytochemistry.

2.3.1. Immunocytochemistry

Neurons were washed in phosphate-buffered saline and then fixed in either 4% formaldehyde/4% sucrose in phosphate-buffered saline for 10 minutes at room temperature followed by incubation in methanol prechilled to −20°C for 10 minutes at 4°C or in methanol (−20°C) only for 20 minutes at 4°C. Fixed neurons were then permeabilized and blocked simultaneously (2% nonimmune goat serum, Sigma, and 0.2% Triton X-100) before incubation in primary antibodies overnight and subsequent incubation with secondary antibodies the following day [20]. In the green/purple color scheme, colocalization is indicated by white overlap.

2.4. Antibodies used

The following antibodies were used: GFP, chicken polyclonal (ab13972; Abcam); PSD95, mouse monoclonal

(clone K28/43; 73-028; NeuroMab); PSD-95, rabbit polyclonal (2507; Cell Signaling Technology); Bassoon, mouse monoclonal (ab82958; Abcam); and GluA1, rabbit polyclonal (ABN241; Millipore).

2.5. Spine morphology and immunofluorescence

Images were acquired with a Leica SP-5 confocal microscope using a $63\times$ oil-immersion objective (Leica, N.A. 1.4) as z-series. Two-dimensional maximum projection reconstructions of images were generated, and morphometric analysis (spine number, area, and breadth) was performed using MetaMorph software (Universal Imaging Corporation, West Chester, PA, USA) [20]. Morphometric analysis was performed on spines from at least two dendrites (secondary or tertiary branches), totaling 100 μm in length, per neuron. For each condition, 9 to 12 neurons from at least three separate experiments (each performed in duplicate) were used. Experiments were carried out blind to condition. Linear density and total gray value of each synaptic protein cluster was measured automatically using MetaMorph [20]. Cultures undergoing direct comparison were stained simultaneously and imaged with the same acquisition parameters.

2.6. Pharmacodynamics

Fasudil and hydroxyfasudil were administered separately at 10, 30, and 100 mg/kg by intraperitoneal (IP) injection to young adult male CD1 mice. Animals were sacrificed 20 minutes after dosing and terminal plasma and brain samples were taken. Proteins were extracted using acetonitrile precipitation, and fasudil and hydroxyfasudil levels were measured by UHPLC-TOF mass spectrometry using electrospray ionization.

2.7. Behavioral testing

2.7.1. Animals

Female Lister Hooded rats (Charles River, UK; weighing $\sim 215 \pm 20$ g at the start of experimentation) were housed in groups of five in individually ventilated two-story home cages, on a 12 hours light cycle (illuminated 07:00–19:00 hours) with controlled temperature $(21 \pm 2°C)$ and humidity $(55 \pm 5\%)$. Water and food (Special Diet Services, UK) were given ad libitum. All experiments were undertaken during the illuminated period and conducted in accordance with UK Animals (Scientific Procedures) 1986 Act and the University of Manchester ethical guidelines.

2.7.2. AβO preparation

Biotin-$A\beta_{1-42}$ (ANA24640) was purchased from Anaspec, USA, disaggregated in hexafluoroisopropanol for 1 hour, aliquoted, hexafluoroisopropanol removed by evaporation under N_2, and monomeric peptide solublized in DMSO at 1 mM, diluted to 100 μM in Ham's F12, and allowed to oligomerize at room temperature for 16 hours.

2.7.3. Surgical procedure

Rats were anesthetized using 4% isoflurane in O_2 in an induction chamber, mounted in a stereotaxic frame and anesthesia maintained with 2% to 3% isoflurane. Ten microliters of 100 μM AβO was injected into the left lateral ventricle using Bregman coordinates, H-0.8, Tr-1.5, V-4.5, at a flow rate of 2.5 μL/minutes (total administered = 10 μmol). Surgery date was defined as day 0. Rats were treated with IP injections of vehicle or fasudil at 10 mg/kg twice daily from days −1 to 6. The novel object recognition test was performed on day 7 as previously described [22]. In brief, rats were placed in a $52 \times 52 \times 51$ cm PVC arena for 3 minutes with two identical objects. Animals were taken out of the box for an intertrial interval of 1 minute, then placed back in the same box for a further 3 minutes with an identical copy of the previous object and a novel object. Both sessions were digitally recorded and the time spent exploring each object scored. The discrimination index was calculated as (novel − familiar)/(novel + familiar).

2.8. Statistical analyses

Statistical analyses were performed in GraphPad or SPSS. Differences in quantitative immunofluorescence, dendritic spine number, and morphology were identified by Student's unpaired *t*-tests. For comparisons between multiple conditions the main effects and simple effects were probed by one-way or two-way analysis of variance with Tukey's correction for multiple comparisons. Error bars represent standard errors of the mean.

3. Results

3.1. Aβ drives Dkk1 production

Aβ drives Dkk1 expression [4,16,23], and Dkk1 protein levels are raised in the brains of Aβ/APP-based mouse models of AD pathology [24]. We extend these observations by showing that increases in both Dkk1 messenger RNA and protein are readily detectable in cultured rodent neurons after treatment with the active portion of Aβ, $A\beta_{25-35}$, and by soluble AβO within 2 to 3 hours, and within 4 hours by AβO at nanomolar concentrations (Fig. 1A and B).

3.2. Synaptic effects of Aβ and Dkk1 are similar

To compare the synaptic effects of Aβ and Dkk1 protein, rat cortical neurons (24 DIV) were transfected with eGFP and 48 hours later treated with either 2 μM AβO for 4 hours or with 400 ng/mL recombinant Dkk1 protein for 3 hours. The additional 1 hour given for Aβ treatments was to allow time for endogenous Dkk1 expression, thereby rendering the two treatments more comparable. AβO and Dkk1 had potent, significant, and very similar
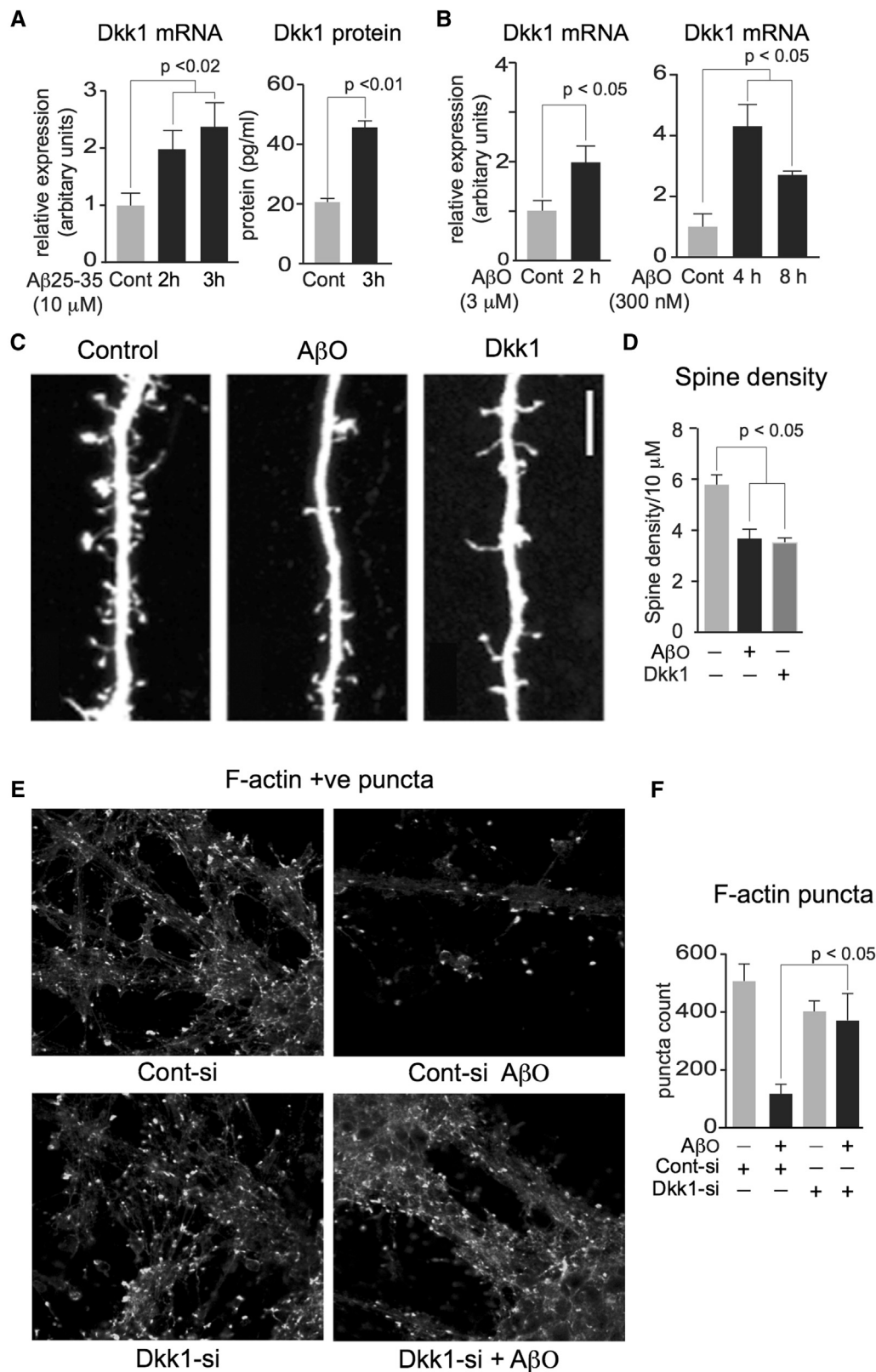
Fig. 1. Aβ synaptotoxicity is Dkk1 dependent. (A) Rat primary cortical neuronal cultures (14 DIV) were treated with 10 μM Aβ$_{25-35}$ for 2 and 3 hours, cells harvested for RNA extraction, and media collected for protein analysis. Complementary DNA was generated and qRT-PCR performed to determine rat Dkk1 mRNA levels (left). Secreted Dkk1 protein levels in media were measured by enzyme-linked immunosorbent assay (right). (B) Similar cultures were treated at 3 μM and 300 nM with an Aβ$_{1-42}$ oligomer (AβO) preparation for the times indicated and harvested and Dkk1 mRNA levels were determined as mentioned previously (C–E). Similar cultures were transfected with eGFP at 24 DIV, 48 hours later treated for 4 hours with 2 μM AβO, or for 3 hours

effects on dendritic spine linear density (Fig. 1C and D). After exposure to either AβO or Dkk1, a small number of immature filopodia-like dendritic spines appear to be spared indicating that Aβ-driven spine loss is selectively targeting dendritic spines with established postsynaptic densities, something we are now investigating in more detail.

3.3. Aβ synaptotoxicity is Dkk1 dependent

Antibody neutralization of Dkk1 blocks Aβ-induced synapse loss [16]. To extend this, we knocked down Dkk1 expression in primary cortical neuronal cultures using a previously validated penetrating peptide-coupled small interfering RNA (siRNA) duplex targeting rat Dkk1 with a scrambled form as control [4]. Assessing synapse number by phalloidin-488 labeling of F-actin puncta in the presence of the control siRNA, 2 μM AβO caused a substantial and significant reduction in synapse number in more than 4 hours. This was significantly blocked in neurons treated with the Dkk1 siRNA (Fig. 1E and F), confirming that Dkk1 is required for Aβ synaptotoxicity to occur.

3.4. Dkk1 synaptotoxicity is Daam1 dependent

Activation of the Wnt-PCP/RhoA/ROCK pathway requires an interaction between Disheveled and Daam1 or Daam2 (Fig. 2A). The only known role of Daam1 and Daam2 is that within the Wnt-PCP pathway [25–27]. To determine if Dkk1-driven synapse loss is Wnt-PCP dependent we individually knocked down DAAM1 and DAAM2 in rat primary cortical cultures using penetrating siRNA duplexes against each. Western blotting of treated cultures demonstrates that only Daam1 is expressed at detectable levels in these cells and that the DAAM1 siRNA potently reduced Daam1 protein expression (Fig. 2B). Daam1 is the predominant neuronal isoform [28]. Using DAAM2si as a control, 24 DIV cultures were treated with each siRNA for 48 hours and subsequently with recombinant Dkk1 protein (400 ng/mL) or vehicle for 3 hours, fixed and synapse number again assessed by counting of phalloidin-labeled F-actin puncta. Neither siRNA significantly affected puncta count compared with untreated control subjects, Dkk1 substantially reduced puncta after DAAM2 siRNA treatment but had no effect after DAAM1 siRNA treatment (Fig. 2C and D). Consistent with this observation the overexpression of Daam1 reduces the synapse number in hippocampal neurons

in a Rho-dependent fashion [28], whereas Aβ has been shown to increase the expression levels of DAAM1 in human neuroblastoma cells [29].

3.5. Aβ-driven, Dkk1-dependent spine loss is mediated by RhoA/ROCK

Downstream of Daam Wnt-PCP regulates actin cytoskeletal dynamics through RhoA and ROCK [30,31]. Next, we investigated whether pharmacologic inhibition of the RhoA/ROCK pathway would inhibit both AβO-driven and Dkk1-driven spine losses. Cortical cultures were transfected with eGFP at 23 DIV and 48 hours later pretreated with the well characterized ROCK inhibitor, Y-27632, or with vehicle for 30 minutes, and then with 2 μM AβO for 4 hours or with 400 ng/mL Dkk1 recombinant protein for 3 hours. Assessment of dendritic spine linear density showed that Y-27632 blocked both AβO-induced and Dkk1-induced spine losses, with similar potency; Y-27632 alone had no effect on spine number (Fig. 3A and B). Together with Figs. 1C–G and 2C and D these data provide strong evidence that Aβ synaptotoxicity is dependent on Dkk1-driven activation of a Wnt-PCP/Daam1/RhoA/ROCK pathway.

3.6. Dkk1 drives GluA1 and PSD-95 relocation

Acute Aβ exposure causes a reduction in synaptic transmission through the internalization of AMPA receptors [32,33], whereas Dkk1 has been suggested to cause a removal of PSD-95 from synapses [16]. However, whether acute exposure to Dkk1 drives the removal of PSD-95 away from dendritic spines and the internalization of AMPA receptors is not known. To investigate this and determine whether effects on PSD-95 and GluA1-containing AMPA receptors could also be blocked by ROCK inhibition, 26 DIV eGFP-expressing cortical neurons were pretreated with Y-27632 or vehicle and subsequently by Dkk1 for 3 hours. After fixation and immunolabeling for PSD-95 and GluA1, confocal imaging revealed that Dkk1 treatment causes a significant reduction in the total number of PSD-95 positive puncta, with significantly fewer PSD-95 positive spines, although concurrently increasing PSD-95 immunoreactive puncta within dendrites. These effects were blocked by Y-27632 (Fig. 3C and D). Dkk1 did not effect the total level of GluA1 puncta but did similarly reduce the number of GluA1 positive spines and increase GluA1 immunolabeling within the dendritic shaft, which was again blocked by Y-27632 (Fig. 3C and E). Dkk1 then, as

with 400 ng/mL Dkk1, fixed, imaged by confocal microscopy, and dendritic spine density and morphology assessed. Both treatments resulted in a significant reduction in dendritic spine linear density (dsld), quantified in (D) (scale bar = 5 μM). Dsld/10 μm: control, 5.8 ± 0.41; AβO, 3.7 ± 0.34; Dkk1, 3.5 ± 0.31; *P* < .001 for all treatments. (E) Examination of average dendritic spine area revealed that AβO and Dkk1 cause a significant reduction in spine area (per μm²): control, 0.85 ± 0.027; AβO, 0.71 ± 0.037; Dkk1, 0.66 ± 0.013; *P* < .01 or *P* < .001. (F and G) Similar cultures were treated overnight with siDkk1 RNA duplex, or a scrambled version as control, each linked to the Pen-1 peptide. Next day cells were treated with 3 μM AβO for 4 hours, fixed, and fluorescently labeled with phalloidin-488, imaged (F), and F-actin labeled puncta quantified (G) (scale bar = 50 μM). In all these significance was determined by ANOVA and Tukey's post hoc *t*-test. Error bars indicate the standard error of the mean. Abbreviations: Aβ, amyloid beta; ANOVA, analysis of variance; DIV, days in vitro; mRNA, messenger RNA.

A

Canonical Wnt
active

Wnt-PCP
active
(canonical inactive)

B

C

F-actin +ve puncta

Control (DAAM2) si

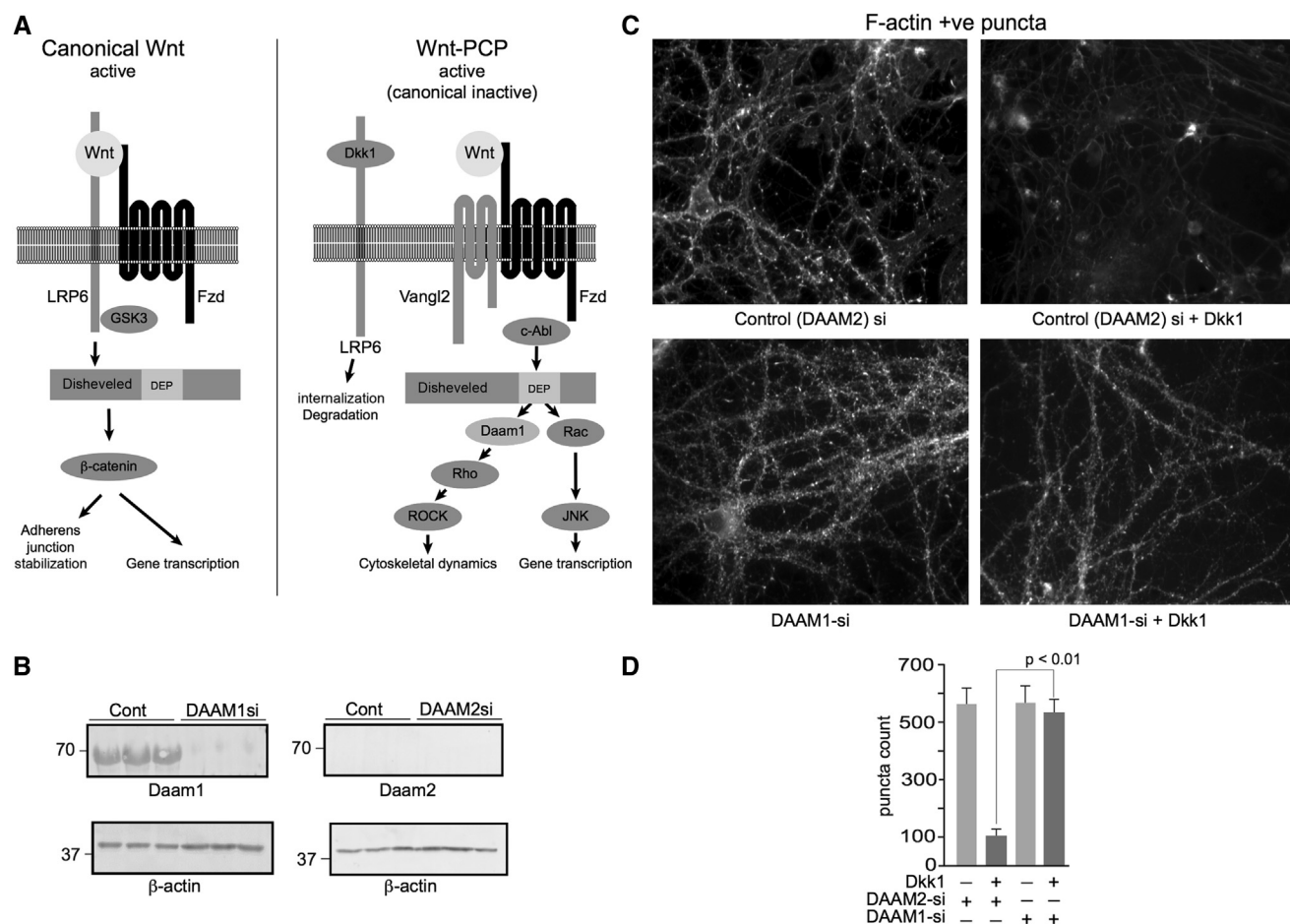Control (DAAM2) si + Dkk1

DAAM1-si

DAAM1-si + Dkk1

D

Fig. 2. Dkk1 synaptotoxicity is Daam1 dependent. (A) Schematic of the Wnt-PCP pathway showing the two arms branching below Disheveled, acting via Daam/Rho/ROCK to regulate cytoskeletal dynamics and JNK/c-Jun primarily to regulate gene transcription. (B) Primary cortical neuronal cultures were treated with DAAM1 or DAAM2 Pen-1–coupled siRNA duplexes for 48 hours, harvested, and analyzed by Western blotting for Daam1 and Daam2. Daam1 was detectable in untreated cells and Daam2 was not. Daam1si potently reduced Daam1 protein expression levels. (C and D) Cultures were treated overnight with DAAM1 or DAAM2 siRNA duplexes. Next day cells were treated with 400 ng/mL recombinant Dkk1 protein for 3 hours, fixed, and fluorescently labeled with phalloidin-488, imaged (C) (scale bar = 50 μM), and F-actin labeled puncta quantified (D). Significance was determined by ANOVA and Tukey's post hoc *t*-test. Error bars indicate the standard error of the mean. Abbreviations: ANOVA, analysis of variance; Dkk1, Dickkopf-1; siRNA, small interfering RNA; Wnt-PCP, Wnt–planar cell polarity.

does Aβ, induces the removal of PSD-95 and GluA1 proteins from synapses and promotes their trafficking into dendrites. This also confirms that Dkk1-induced dendritic spine loss is concomitant with a loss of synapses via a RhoA/ROCK-dependent mechanism.

3.7. Aβ and Dkk1-induced spine withdrawal are blocked by fasudil

To confirm that effects of Y-27632 (hexane carboxamide) are via ROCK we selected a second structurally dissimilar ROCK inhibitor, fasudil (an isoquinoline), one of only two ROCK inhibitors approved for use in man [34]. eGFP expressing cortical cultures were pretreated with 5 μM fasudil or vehicle for 30 minutes and subsequently with either 2 μM AβO or 400 ng/mL Dkk1 recombinant protein, fixed, and imaged by confocal microscopy. Fasudil alone, like Y-27632, had a little effect on spine density. AβO and Dkk1 both significantly reduced spine number

and the effects of each were again blocked by fasudil (Fig. 4A and B). These data support our contention that the synaptic effects of both Aβ and Dkk1 are dependent on the Wnt-PCP/RhoA/ROCK pathway and substantiate the synaptoprotective properties only very recently attributed to fasudil [35].

3.8. Fasudil rescues Aβ-driven cognitive deficits

Because fasudil has clinical approval and protects against Aβ synaptotoxicity make it a promising candidate for repositioning in AD. To further assess its usefulness we examined its ability to protect against AβO-induced cognitive impairment in vivo using a novel acute rat model [36]. Despite the predicted low central nervous system penetrance of fasudil [37], both it [38] and its active metabolite hydroxyfasudil [39] appear to be centrally active after peripheral administration. Given the paucity of data concerning brain availability of either compound and to inform on dosing for in vivo
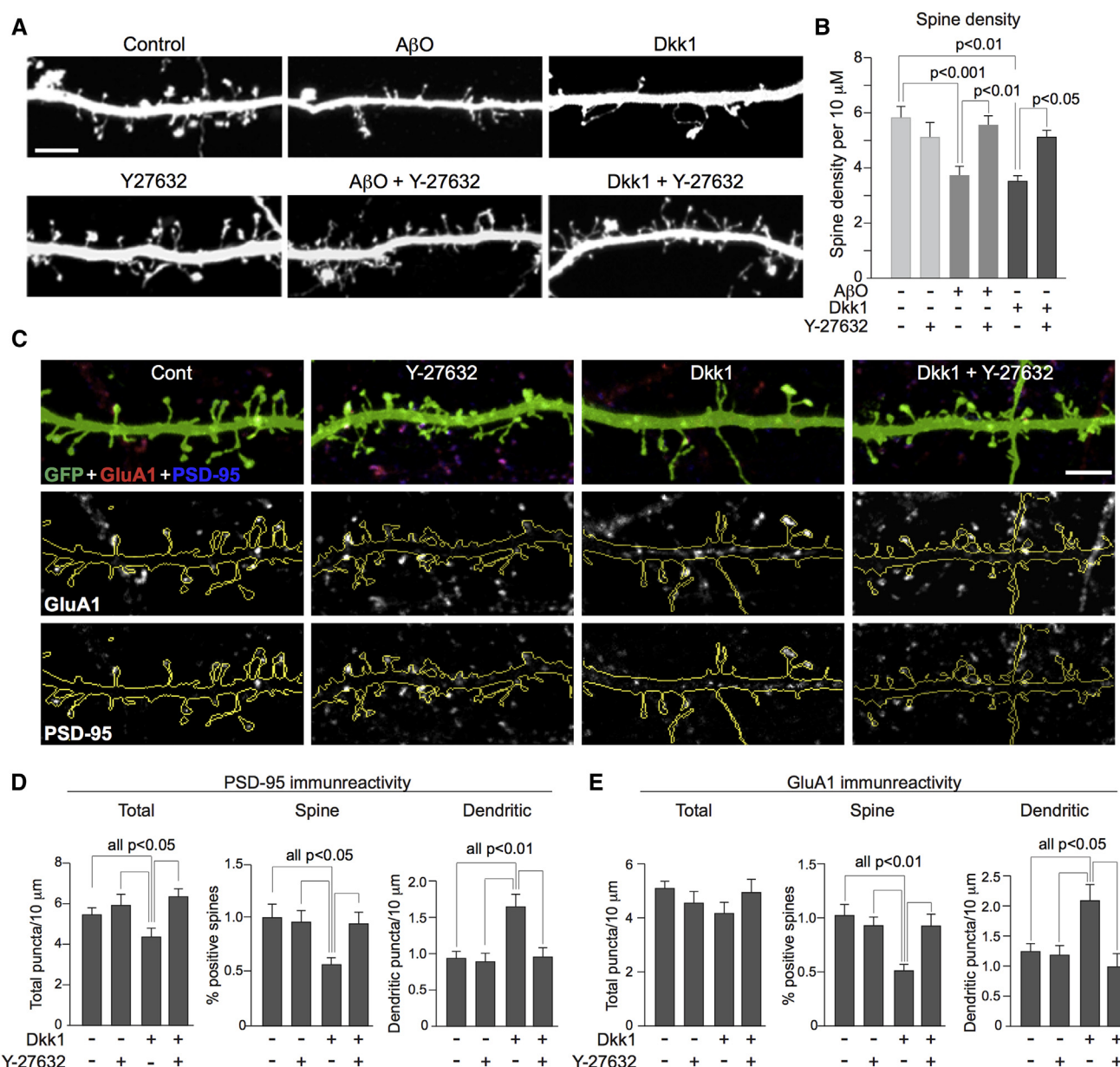
Fig. 3. Aβ and Dkk1 synaptic effects are ROCK dependent. (A and B) Rat primary cortical neurons were transfected with eGFP at 24 DIV and 48 hours later treated with Y27632 or vehicle and 15 minutes later with 2 μM AβO for 4 hours or 400 ng/mL Dkk1 for 3 hours, fixed, and imaged by confocal microscopy for the examination of spine morphology. AβO and Dkk1 caused a significant reduction in dendritic spine linear density. Y2763 alone had no significant effect on spine density but in combination with AβO and Dkk1 blocked the effect of both (scale bar = 5 μM). (C–E) Rat primary 26 DIV neurons expressing eGFP were treated with Y27632 and Dkk1 all as mentioned in (A). Concurrent with a loss of spine density, Dkk1 caused a significant reduction in total PSD-95 puncta (total PSD-95 density/10 μm: control, 5.5 ± 0.34; control + Y-27632, 6.2 ± 0.55; Dkk1, 4.3 ± 0.39; Dkk1 + Y-27632, 6.6 ± 0.43). Interestingly, the number of spines containing PSD-95 was also reduced, with a concurrent increase in the density of dendritic PSD-95, after treatment with Dkk1. This effect was blocked by Y2763 (% spines containing PSD-95: control, 79.8 ± 2.4; control + Y-27632, 78.2 ± 2.7; Dkk1, 59.1 ± 3.7; Dkk1 + Y-27632, 78.9 ± 2.1). Dendritic PSD-95 puncta/10 μm: control, 0.93 ± 0.11; control + Y-27632, 0.89 ± 0.11; Dkk1, 1.67 ± 0.17; Dkk1 + Y-27632, 0.95 ± 0.15. (E) Dkk1 did not significantly affect the total level of GluA1 immunoreactive puncta but did reduce the number of spines positive for GluA1 and increased levels of GluA1 in dendrites, which was again blocked by inhibition of ROCK. GluA1 linear density/10 μm: control, 5.0 ± 0.34; control + Y-27632, 4.6 ± 0.40; Dkk1, 4.2 ± 0.40; Dkk1 + Y-27632, 4.9 ± 0.44; $P = .4574$; % spines containing GluA1: control, 67.8 ± 4.3; control + Y-27632, 68.4 ± 3.7; Dkk1, 47.9 ± 4.4; Dkk1 + Y-27632, 65.6 ± 3.1. Dendritic GluA1 puncta/10 μm: control, 1.25 ± 0.13; control + Y-27632, 1.20 ± 0.15; Dkk1, 2.09 ± 0.26; Dkk1 + Y-27632, 0.99 ± 0.22. Abbreviations: Aβ, amyloid beta; AβO, Aβ$_{1-42}$ oligomer; DIV, days in vitro; Dkk1, Dickkopf-1.

experimentation we evaluated brain penetrance of fasudil and hydroxyfasudil. Each was administered at a range of doses intraperitoneally to CD1 mice and levels of each were measured in brain and plasma by mass spectrometry. Data

obtained demonstrate that fasudil is brain penetrant with a plasma:brain ratio of 8.5% at the 10 mg/kg dose (Fig. 4C). This figure is better than that of a number of compounds widely used to treat a number of central nervous system
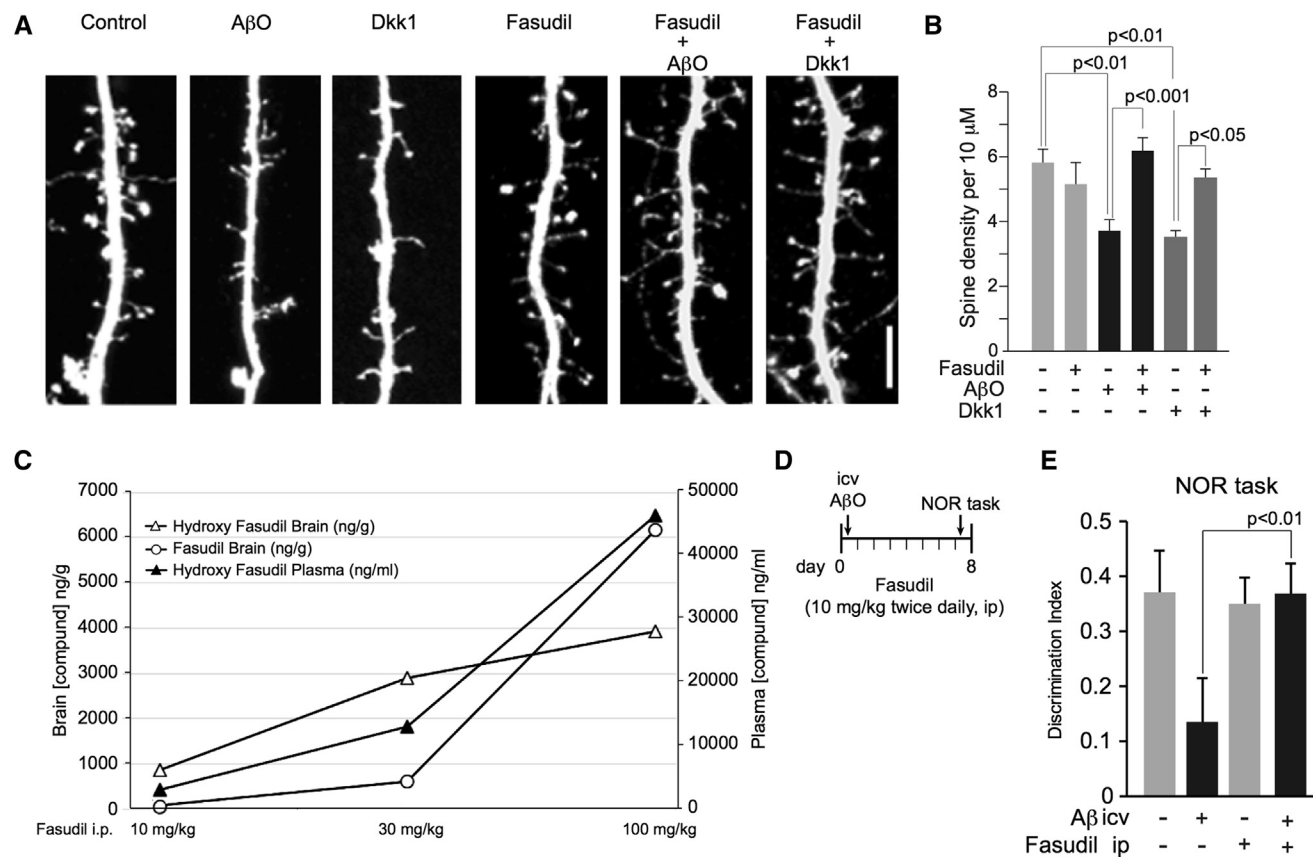
Fig. 4. Fasudil is central nervous system penetrant and blocks Aβ synaptotoxicity and cognitive impairment. (A and B) Rat primary cortical neuronal cultures were transfected with eGFP at 26 DIV and 48 hours later pretreated with 5 μM fasudil or vehicle for 15 minutes and subsequently treated with AβO or Dkk1 and imaged as in (A) (scale bar = 5 μM). AβO and Dkk1 caused a significant reduction in dsld, which fasudil fully and significantly blocked, as shown in (B) (dsld/ 10 μm: control, 5.8 ± 0.41; fasudil, 5.2 ± 0.64; AβO, 3.7 ± 0.34; AβO + fasudil, 6.2 ± 0.38; Dkk1, 3.5 ± 0.20; Dkk1 + fasudil, 5.4 ± 0.27). (B) Significance determined by ANOVA and Tukey's post hoc *t*-test. Error bars indicate the standard deviation. (C) Male CD1 mice were administered fasudil or hydroxyfasudil **Q25** at 10, 30, and 100 mg/kg, IP and brain and plasma collected 20 minutes after injection. Fasudil and hydroxyfasudil were detected and measured by mass spectrometry. (D and E) Forty young adult female rats were administered 10 mg/kg fasudil, or vehicle, IP, twice daily for 7 days, and given either a single dose of AβO or vehicle, unilaterally, intracerebroventricularly on day 1. On day 7, all animals were presented with a NOR task, schematized in (D). Rats receiving vehicle and AβO showed profound deficit in this task, whereas the performance of rats receiving AβO and fasudil was not different to that of control subjects (E). Abbreviations: Aβ, amyloid beta; AβO, Aβ$_{1-42}$ oligomer; DIV, days in vitro; Dkk1, Dickkopf-1; dsld, dendritic spine linear density; IP, intraperitoneal; NOR, novel object recognition.

disorders such as clozapine (1.1%), haloperidol (1.1%), and diazepam (3.6%) and is similar to that of donepezil, 12.6% [40], one of the few drugs currently licensed for AD.

On the basis of these data 40 adult female rats of 250 to 300 g body weight were administered fasudil (10 mg/kg) or vehicle (saline) intraperitoneally twice daily for 7 days. After the initial IP injection, all animals underwent surgery on day 1 to receive a single intracranial injection into the left lateral ventricle of either 10 nmol AβO or vehicle in a volume of 10 μL (at 2.5 μL/minutes) resulting in four groups (n = 10/group). On day 7, all 40 animals were presented with a novel object recognition (NOR) task as previously described [41]. In rats receiving vehicle the single dose of AβO produced a marked and highly significant impairment in NOR performance compared with control subjects. Fasudil alone had no effect on NOR performance but completely rescued performance deficits because of AβO (Fig. 4C). These data confirm that peripherally administered fasudil

is able to block AβO-driven cognitive impairment. Given the supporting evidence presented previously, we propose that fasudil is able to protect against Aβ-induced cognitive impairment through its ability to antagonize an Aβ activated Dkk1/Wnt-PCP/Daam1/RhoA/ROCK-dependent pathway that drives dendritic spine withdrawal and synapse loss.

4. Discussion

Opposing roles for the canonical and noncanonical Wnt signaling pathways in synapse homeostasis have been previously recognized, with canonical Wnt promoting synapse formation and stabilization [42] and noncanonical promoting synapse disassembly/pruning [43,44]. Under normal physiological conditions both pathways likely act in a highly regulated and concerted manner to achieve the appropriate levels of synaptic plasticity and resultant cognitive functioning to occur. Inappropriate levels of Aβ
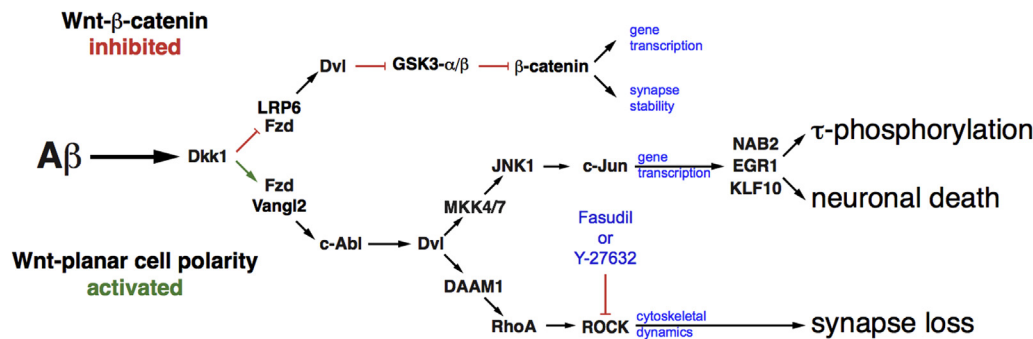
Fig. 5. Schematic of Aβ-driven Wnt-PCP pathway activation. Aβ drives a rapid increase in Dkk1 expression. Concomitant with antagonism of canonical Wnt–β-catenin signaling Dkk1 then drives the activation of the Wnt-PCP pathway by antagonizing the LRP6-Fzd interaction. We have previously shown that activity in the JNK/c-Jun arm of Wnt-PCP induces the expression of several identified genes required for Aβ-driven increases in tau phosphorylation and neuronal death to occur. Here, we demonstrate that activity of the Daam1/RhoA/ROCK arm is necessary for Aβ-driven synaptotoxicity and that this can be blocked by ROCK inhibitors Y27632 or fasudil. Abbreviations; Aβ, amyloid beta; c-Abl1, c-Abl oncogene 1, nonreceptor tyrosine kinase (ABL1); c-Jun (JUN), ■; DAAM1, disheveled-associated activator of morphogenesis 1; Dkk1, Dickkopf-1; Dvl, disheveled; EGR1, early growth response 1; Fzd, frizzled; GSK3-α/β, glycogen synthase kinase-α/β; JNK1, c-Jun N-terminal kinase (MAPK8); KLF10, Krüppel-like factor 10; LRP6, LDL receptor related protein 6; MKK4/7, mitogen-activated protein kinase kinase 4/7 (MAP2K4 and MAP2K7); NAB2, NGFI-A binding protein 2; RhoA, ras homolog family member A; ROCK, rho-associated coiled-coil containing protein kinase; PCP, planar cell polarity; Vangl2, Van Gogh-like protein 2.

result in cognitive impairment and memory deficits by disrupting these processes.

Our data demonstrate that Aβ-driven synapse withdrawal involves the Dkk1-dependent activation of the Wnt-PCP/RhoA/ROCK pathway. We show that at nanomolar levels, oligomeric forms of Aβ$_{1-42}$ regarded to be the most synaptotoxic form of Aβ [45,46] rapidly upregulate neuronal Dkk1 expression, leading to dendritic spine retraction and altered localization of the postsynaptic proteins, PSD-95 and GluA1, in a Daam1-dependent and ROCK-dependent manner.

It has been postulated that Dkk1 alters synapse stability predominantly through antagonism of the canonical Wnt–β-catenin pathway [16], which will contribute to the process given the role of canonical Wnt in synapse formation and stability [42,47]. Our data significantly advance on this idea, demonstrating that Dkk1-mediated synapse loss involves the simultaneous and necessary activation of the Wnt-PCP/RhoA/ROCK pathway. This is in line with previous reports specifically pointing to a role of Wnt-PCP in synapse disassembly through core PCP component, Vangl2 [43,44].

We previously reported that Aβ, through Dkk1, aberrantly activates the JNK/c-Jun arm of Wnt-PCP, and this then drives the expression of genes required for Aβ-induced neuronal death and increases in tau phosphorylation in vitro and in vivo [4]. Furthermore, we also presented evidence that the signaling pathways most associated with disease in the AD brain are shaped, if not driven by Dkk1/Wnt-PCP activity [4]. We now argue then that the Aβ-driven Dkk1-dependent activation of Wnt-PCP underpins several of the key neuropathologic characteristic of AD, including possibly the most fundamental of all, synapse loss. This concept is depicted schematically in Fig. 5. Given the familial AD gene, APP, the Aβ parent molecule, has itself recently been shown to be a modulatory

component of the Wnt-PCP coreceptor complex [48], surely underpins the importance of this pathway in the disease process and indicates that a better understanding of the roles of both Aβ and APP in it, will shed further light on the process and our ability to intervene therapeutically to slow it down or prevent it.

Here, not only do we shed new light on these mechanisms but have also identified fasudil, a drug approved for clinical use in Japan and China since 1994 for cerebrovascular vasospasm, as a strong candidate for repositioning/repurposing in AD. We assessed the pharmacodynamics of fasudil and its active metabolite hydroxyfasudil and found that both have good brain penetrance. Because of legal infringements within the pharmaceutical industry fasudil has not received the Food and Drug Administration or European approval. However, in China it has been used in a small clinical trial in patients with AD in combination with a second vasodilator, nimodipine, and in this study, based on the cognitive assessment, was found to give benefit compared with nimodipine alone [49].

Given the recent report that ROCK inhibitor Y-27632 can reverse Dkk1-induced synapse loss in vivo [47] and that fasudil is a well tolerated in man [50], the data we present here concerning its ability to protect against Aβ synaptotoxicity, to be brain penetrant, and to protect against Aβ-induced cognitive impairment warrant serious assessment of its utility as a much needed treatment for AD.

References

[1] Vargas LM, Leal N, Estrada LD, Gonzalez A, Serrano F, Araya K, et al. EphA4 activation of c-Abl mediates synaptic loss and LTP blockade caused by amyloid-beta oligomers. PLoS One 2014;9:e92309.

[2] Pozueta J, Lefort R, Shelanski ML. Synaptic changes in Alzheimer's disease and its models. Neuroscience 2013;251:51–65.

[3] Lambert MP, Barlow AK, Chromy BA, Edwards C, Freed R, Liosatos M, et al. Diffusible, nonfibrillar ligands derived from Abeta1-42 are potent central nervous system neurotoxins. Proc Natl Acad Sci U S A 1998;95:6448–53.

[4] Killick R, Ribe EM, Al-Shawi R, Malik B, Hooper C, Fernandes C, et al. Clusterin regulates beta-amyloid toxicity via Dickkopf-1-driven induction of the Wnt-PCP-JNK pathway. Mol Psychiatry 2014;19:88–98.

[5] Bafico A, Liu G, Yaniv A, Gazit A, Aaronson SA. Novel mechanism of Wnt signalling inhibition mediated by Dickkopf-1 interaction with LRP6/Arrow. Nat Cell Biol 2001;3:683–6.

[6] Povelones M, Howes R, Fish M, Nusse R. Genetic evidence that Drosophila frizzled controls planar cell polarity and Armadillo signaling by a common mechanism. Genetics 2005;171:1643–54.

[7] Huang Y, Sun X, Hu G. An integrated genetics approach for identifying protein signal pathways of Alzheimer's disease. Comput Methods Biomech Biomed Engin 2011;14:371–8.

[8] Salinas PC. Synaptogenesis: Wnt and TGF-beta take centre stage. Curr Biol 2003;13:R60–2.

[9] Brigidi GS, Bamji SX. Cadherin-catenin adhesion complexes at the synapse. Curr Opin Neurobiol 2011;21:208–14.

[10] Seong E, Yuan L, Arikkath J. Cadherins and catenins in dendrite and synapse morphogenesis. Cell Adh Migr 2015;9:202–13.

[11] Viola KL, Velasco PT, Klein WL. Why Alzheimer's is a disease of memory: the attack on synapses by A beta oligomers (ADDLs). J Nutr Health Aging 2008;12:51S–7.

[12] Penzes P, Cahill ME, Jones KA, VanLeeuwen JE, Woolfrey KM. Dendritic spine pathology in neuropsychiatric disorders. Nat Neurosci 2011;14:285–93.

[13] Terry RD, Masliah E, Salmon DP, Butters N, DeTeresa R, Hill R, et al. Physical basis of cognitive alterations in Alzheimer's disease: synapse loss is the major correlate of cognitive impairment. Ann Neurol 1991; 30:572–80.

[14] Selkoe DJ. Alzheimer's disease is a synaptic failure. Science 2002; 298:789–91.

[15] Bellot A, Guivernau B, Tajes M, Bosch-Morato M, Valls-Comamala V, Munoz FJ. The structure and function of actin cytoskeleton in mature glutamatergic dendritic spines. Brain Res 2014;1573:1–16.

[16] Purro SA, Dickins EM, Salinas PC. The secreted Wnt antagonist Dickkopf-1 is required for amyloid beta-mediated synaptic loss. J Neurosci 2012;32:3492–8.

[17] Schratt G. microRNAs at the synapse. Nat Rev Neurosci 2009; 10:842–9.

[18] Ethell IM, Pasquale EB. Molecular mechanisms of dendritic spine development and remodeling. Prog Neurobiol 2005;75:161–205.

[19] Salminen A, Suuronen T, Kaarniranta K. ROCK, PAK, and Toll of synapses in Alzheimer's disease. Biochem Biophys Res Commun 2008; 371:587–90.

[20] Srivastava DP, Woolfrey KM, Penzes P. Analysis of dendritic spine morphology in cultured CNS neurons. J Vis Exp 2011;e2794.

[21] Xie Z, Srivastava DP, Photowala H, Kai L, Cahill ME, Woolfrey KM, et al. Kalirin-7 controls activity-dependent structural and functional plasticity of dendritic spines. Neuron 2007;56:640–56.

[22] McLean SL, Idris NF, Woolley ML, Neill JC. D(1)-like receptor activation improves PCP-induced cognitive deficits in animal models: implications for mechanisms of improved cognitive function in schizophrenia. Eur Neuropsychopharmacol 2009;19:440–50.

[23] Caricasole A, Copani A, Caraci F, Aronica E, Rozemuller AJ, Caruso A, et al. Induction of Dickkopf-1, a negative modulator of the Wnt pathway, is associated with neuronal degeneration in Alzheimer's brain. J Neurosci 2004;24:6021–7.

[24] Rosi MC, Luccarini I, Grossi C, Fiorentini A, Spillantini MG, Prisco A, et al. Increased Dickkopf-1 expression in transgenic mouse models of neurodegenerative disease. J Neurochem 2010; 112:1539–51.

[25] Lee HK, Deneen B. Daam2 is required for dorsal patterning via modulation of canonical Wnt signaling in the developing spinal cord. Dev Cell 2012;22:183–96.

[26] Habas R, Kato Y, He X. Wnt/frizzled activation of Rho regulates vertebrate gastrulation and requires a novel Formin homology protein Daam1. Cell 2001;107:843–54.

[27] Ajima R, Bisson JA, Helt JC, Nakaya MA, Habas R, Tessarollo L, et al. DAAM1 and DAAM2 are co-required for myocardial maturation and sarcomere assembly. Dev Biol 2015;408:126–39.

[28] Salomon SN, Haber M, Murai KK, Dunn RJ. Localization of the diaphanous-related formin Daam1 to neuronal dendrites. Neurosci Lett 2008;447:62–7.

[29] Morte B, Martinez T, Zambrano A, Pascual A. Monocyte-mediated regulation of genes by the amyloid and prion peptides in SH-SY5Y neuroblastoma cells. Neurochem Int 2011;58:613–9.

[30] Phillips HM, Murdoch JN, Chaudhry B, Copp AJ, Henderson DJ. Vangl2 acts via RhoA signaling to regulate polarized cell movements during development of the proximal outflow tract. Circ Res 2005;96:292–9.

[31] Winter CG, Wang B, Ballew A, Royou A, Karess R, Axelrod JD, et al. Drosophila Rho-associated kinase (Drok) links Frizzled-mediated planar cell polarity signaling to the actin cytoskeleton. Cell 2001; 105:81–91.

[32] Hsieh H, Boehm J, Sato C, Iwatsubo T, Tomita T, Sisodia S, et al. AMPAR removal underlies Abeta-induced synaptic depression and dendritic spine loss. Neuron 2006;52:831–43.

1341 [33] Guntupalli S, Widagdo J, Anggono V. Amyloid-beta-induced dysregu-
1342   lation of AMPA receptor trafficking. Neural Plast 2016;2016:3204519.
1343 [34] Feng Y, LoGrasso PV, Defert O, Li R. Rho Kinase (ROCK) inhibitors
1344   and their therapeutic potential. J Med Chem 2016;59:2269–300.
1345 [35] Yu JZ, Chen C, Zhang Q, Zhao YF, Feng L, Zhang HF, et al. Changes
1346   of synapses in experimental autoimmune encephalomyelitis by using
1347   Fasudil. Wound Repair Regen 2016;24:317–27.
1348 [36] Daniels MJ, Rivers-Auty J, Schilling T, Spencer NG, Watremez W,
1349   Fasolino V, et al. Fenamate NSAIDs inhibit the NLRP3 inflammasome
1350   and protect against Alzheimer's disease in rodent models. Nat Com-
1351   mun 2016;7:12504.
1352 [37] Valdivia AC, Mason S, Collins J, Buckley KR, Coletta P,
1353   Beanlands RS, et al. Radiosynthesis of N-[(11)C]-methyl-hydroxyfa-
1354   sudil as a new potential PET radiotracer for rho-kinases (ROCKs).
1355   Appl Radiat Isot 2010;68:325–8.
1356 [38] Song Y, Chen X, Wang LY, Gao W, Zhu MJ. Rho kinase inhibitor fa-
1357   sudil protects against beta-amyloid-induced hippocampal neurodegen-
1358   eration in rats. CNS Neurosci Ther 2013;19:603–10.
1359 [39] Huentelman MJ, Stephan DA, Talboom J, Corneveaux JJ,
1360   Reiman DM, Gerber JD, et al. Peripheral delivery of a ROCK inhibitor
1361   improves learning and working memory. Behav Neurosci 2009;
1362   123:218–23.
1363 [40] Summerfield SG, Read K, Begley DJ, Obradovic T, Hidalgo IJ,
1364   Coggon S, et al. Central nervous system drug disposition: the relation-
1365   ship between in situ brain permeability and brain free fraction. J Phar-
1366   macol Exp Ther 2007;322:205–13.
1367 [41] McLean SL, Grayson B, Marsh S, Zarroug SH, Harte MK, Neill JC.
1368   Nicotinic alpha7 and alpha4beta2 agonists enhance the formation
1369   and retrieval of recognition memory: potential mechanisms for

cognitive performance enhancement in neurological and psychiatric
disorders. Behav Brain Res 2016;302:73–80.
[42] Stamatakou E, Salinas PC. Postsynaptic assembly: a role for Wnt
signaling. Dev Neurobiol 2013;74:818–27.
[43] Thakar S, Wang L, Yu T, Ye M, Onishi K, Scott J, et al. Evidence for
opposing roles of Celsr3 and Vangl2 in glutamatergic synapse forma-
tion. Proc Natl Acad Sci U S A 2017;114:E610–8.
[44] Nagaoka T, Ohashi R, Inutsuka A, Sakai S, Fujisawa N, Yokoyama M,
et al. The Wnt/planar cell polarity pathway component Vangl2 induces
synapse formation through direct control of N-cadherin. Cell Rep
2014;6:916–27.
[45] Walsh DM, Selkoe DJ. A beta oligomers—a decade of discovery. J
Neurochem 2007;101:1172–84.
[46] Tu S, Okamoto S, Lipton SA, Xu H. Oligomeric Abeta-induced synap-
tic dysfunction in Alzheimer's disease. Mol Neurodegener 2014;9:48.
[47] Marzo A, Galli S, Lopes D, McLeod F, Podpolny M, Segovia-
Roldan M, et al. Reversal of synapse degeneration by restoring Wnt
signaling in the adult hippocampus. Curr Biol 2016;26:2551–61.
[48] Soldano A, Okray Z, Janovska P, Tmejova K, Reynaud E, Claeys A,
et al. The Drosophila homologue of the amyloid precursor protein is
a conserved modulator of Wnt PCP signaling. PLoS Biol 2013;
11:e1001562.
[49] Bin Y, Fang S, Li-hui D, Qiao-ling P, Wen-xin Z, Guo-qing Z. Curative
effect of Fasudil injection combined with Nimodipine on Alzheimer
disease of elderly patients. J Clin Med Pract 2011;14.   Q23
[50] Jiang R, Ai ZS, Jiang X, Yuan P, Liu D, Zhao QH, et al. Intravenous
fasudil improves in-hospital mortality of patients with right heart fail-
ure in severe pulmonary hypertension. Hypertens Res 2015;
38:539–44.